

RESEARCH ARTICLE

OVERCOMING DEAD TIME IN THERMAL PROCESSES: A COMPARATIVE EVALUATION OF PID-SP AND PID-IMC CONTROL STRATEGIES

Yulius Deddy Hermawan^{a*}, Yusmardhany Yusuf^a, Joko Pamungkas^b, Brian Rizky Fardhiansyah^a, Alifya Dinda Aditya^a, Hanum Mizati^a, Hasabneya Primaputra Artahsasta^a

^a Department of Chemical Engineering, Faculty of Industrial Engineering, Universitas Pembangunan Nasional "Veteran" Yogyakarta, Yogyakarta, Indonesia

^b Department of Petroleum Engineering, Faculty of Mineral Technology and Energy, Universitas Pembangunan Nasional "Veteran" Yogyakarta, Yogyakarta, Indonesia

*Corresponding Author E-mail: ydhermawan@upnyk.ac.id

This is an open access article distributed under the Creative Commons Attribution License CC BY 4.0, which permits unrestricted use, distribution, and reproduction in any medium, provided the original work is properly cited.

ARTICLE DETAILS

Article History:

Received 17 September 2025
Revised 18 October 2025
Accepted 20 November 2025
Available online 25 December 2025

ABSTRACT

Dead time is a major source of instability and performance loss in process control systems, requiring effective compensation strategies. This study investigates temperature regulation in a two-tank thermal system with transport delay using two control configurations: PID with Smith Predictor (PID-SP) and PID with Internal Model Control (PID-IMC). A 10 L laboratory-scale stirred-tank heater was modeled as a first-order-plus-dead-time (FOPDT) process, and controller parameters were tuned using the Process Reaction Curve (PRC) method. Closed-loop simulations in Scilab/XCOS were performed for both regulatory and servo control cases under various delay conditions. The results show that PID-IMC achieves faster settling, smaller integral absolute error (IAE), and smoother manipulated-variable responses, while PID-SP offers better robustness to delay variations. The key finding highlights that PID-IMC provides higher precision for well-modeled processes, whereas PID-SP ensures stable performance under model uncertainty. These insights are valuable for improving process control design and implementation in industrial thermal systems with significant dead time.

KEYWORDS

Dead time, IMC, PID, Smith-predictor, thermal system

1. INTRODUCTION

From a process control perspective, pure delay, or dead time, is a major source of instability. As noted, larger dead times make processes increasingly difficult to control and often lead to unstable responses (Stephanopoulos, 1984). Dead time is the delay between an input change and its effect, often occurring in multi-capacity chemical processes. The presence of long connecting pipes introduces significant dead time, causing a delayed response of the output to input changes (Marlin, 1995). Therefore, investigating the dynamics and control of the process system with dead time is essential for improving process stability and performance.

Luyben emphasized that proper tuning of proportional-integral-derivative (PID) parameters is essential for process stability (Luyben, 2002). Although PID tuning methods such as the process reaction curve (PRC) and open-loop on-off test have been successfully applied in laboratory-scale systems, their potential for addressing dead-time challenges in thermal processes remains underexplored (Hermawan and Haryono, 2012; Alvaro et al., 2018; Hermawan and Puspitasari, 2018). Prior studies confirmed that properly tuned PID controllers outperform P and PI controllers by producing stable, rapid, and robust responses (Hermawan and Haryono, 2012; Hermawan and Puspitasari, 2018). This study extends those findings by evaluating integrated PID-Smith predictor (PID-SP) and PID-Internal Model Control (PID-IMC) strategies, offering new insights into practical dead-time compensation for process industries.

Conventional methods such as the Smith Predictor and its variants have been applied to mitigate dead time in process systems (Kravaris and Wright, 1989; Stojic et al., 2001; Panda et al., 2006; Juneja et al., 2010). While effective, they often struggle with robustness and practical implementation. This study addresses that gap by evaluating integrated PID-IMC and PID-SP strategies as practical and reliable alternatives for dead-time compensation in thermal processes.

This research focuses on temperature control of a 10 L laboratory-scale stirred-tank heater with significant dead time, combining experimental validation and dynamic simulation. PID parameters were initially tuned using the PRC method, and both PID-SP and PID-IMC strategies were implemented using Scilab/XCOS to evaluate closed-loop performance under various operating conditions. By integrating model-based analysis with practical implementation, this study provides a comprehensive evaluation of dead-time compensation strategies and demonstrates the superior precision and control performance of PID-IMC compared to conventional approaches, contributing valuable insights for industrial process control design.

2. LITERATURE REVIEW

Dead time (also referred to as time delay) is a fundamental challenge in process control because it causes the system output to lag behind the input by a fixed duration. This delay arises naturally in many thermal and chemical processes due to transport lags, sensor delays, and actuator dynamics (Stephanopoulos, 1984; Smith and Corripio, 1997; Seborg et al., 2017). In the

Quick Response Code



Access this article online

Website:
www.gwk.com.my

DOI:
10.26480/gwk.02.2025.51.59

frequency domain, dead time introduces an exponential factor e^{-tDs} that contributes significant phase lag, reducing stability margins and complicating the design of conventional feedback controllers such as PID. Without appropriate compensation, systems with dead time often exhibit sluggish responses, oscillations, or even instability when controlled using standard methods (Kravaris, 1989; Stojic et al., 2001; Panda et al., 2006; Karan and Dey, 2023; Hermawan et al., 2024).

The Smith Predictor (SP), first proposed by remains one of the most established methods for dead-time compensation (Smith, 1957). By using a process model, the SP predicts the process output as if no delay were present, thereby restoring effective feedback action. Although highly effective when the model is accurate, the SP is sensitive to mismatches in process dynamics or delay estimation. To overcome this limitation, extensions like the Analytical Predictor, Inferential Control, and Internal Model Control (IMC) were developed, sharing a common mathematical basis but offering alternative design perspectives (Kravaris and Wright, 1989).

In recent years, several modern methods to handle dead time have been developed, especially combining modified SP (MSP) structures with IMC-based tuning. For example, an MSP with IMC tuning was proposed for second-order, delay-dominated processes and processes with right-half plane (RHP) dynamics, showing improved setpoint tracking and disturbance rejection with smooth responses and minimal overshoot (Karan and Dey, 2023). In another work, a simple modified Smith predictor was used for integrating time-delayed processes (IPTD), using a sole closed-loop time constant from IMC design to reduce tuning complexity, achieving zero overshoot on setpoint change and fast disturbance recovery (Karan et al., 2022; Divakar et al., 2024). Also, work on fractional-order IMC and Smith Predictor combinations has shown good robustness and performance under parameter variations, especially for integrating and unstable processes with long dead time (Korupu and Muthukumarasamy, 2021).

Modern dead-time compensation methods use a structured design. The process model is divided into a delay-free part, such as FOPDT (Juneja et al., 2010), IPTD (Divakar et al., 2024), or a second-order system with dominant delay (Karan and Dey, 2023; Hermawan et al., 2024). An inner loop, or predictor, typically a Smith predictor or its modified form, compensates for the delay. An outer IMC-based controller or filter then balances performance and robustness through a single tuning parameter, usually the closed-loop time constant. Recent studies enhance these frameworks using fractional-order filters, lead-lag or PD/PI elements, and additional features to improve robustness against model mismatch and disturbances. Collectively, MSP-IMC designs achieve faster stabilization, minimal overshoot, smoother control effort, strong disturbance rejection, and improved robustness against uncertainty.

Despite extensive studies on dead-time compensation, most prior works remain limited to theoretical models or simulations, with few validated experimentally on real thermal systems. Most SP and IMC designs are evaluated under idealized conditions, neglecting the nonlinearities and disturbances present in real processes. Comparative studies of PID-SP and PID-IMC in small-scale thermal systems remain limited, creating a gap between theoretical development and practical performance.

To address this, the present study investigates the control of a 10 L stirred tank heater with dead time through combined laboratory experiments and dynamic simulations. PID parameters were initially tuned using the Process Reaction Curve (PRC) method, while PID-SP and PID-IMC strategies were implemented for dead-time compensation. The system model was analyzed in XCOS to assess closed-loop performance and robustness. The integral absolute error (IAE) criterion was applied to evaluate controller performance. Lower IAE values indicated superior stability, faster settling, and smoother control effort, confirming the method's practicality and robustness for thermal processes with significant dead time.

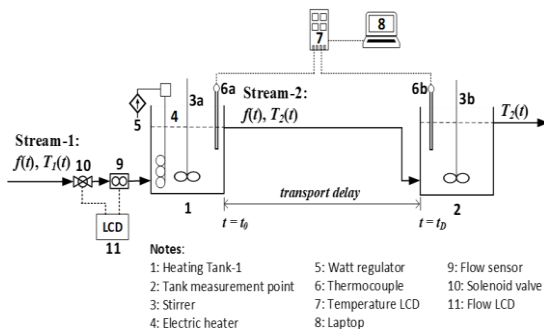


Figure 1: Experimental apparatus setup.

3. RESEARCH METHOD

Figure 1 depicts the experimental setup of the single-tank heating system. Water enters Tank 1 (No. 1) at a flow rate $f(t)$ [L/min] and temperature $T_1(t)$ [°C], where it is heated by an electric heater (No. 4) with power regulated by a watt controller (No. 5) and homogenized by a mechanical stirrer (No. 6a) to ensure uniform temperature distribution. The tank is designed with an overflow system to maintain a constant liquid volume. Water temperatures in Tank 1 and Tank 2 are measured by thermocouples (Nos. 6a and 6b), respectively, where the response in Tank 2 indicates a transportation delay. Temperature readings are displayed on an LCD (No. 7) and recorded on a laptop (No. 8). A flowmeter (No. 9), solenoid valve (No. 10), and LCD (No. 11) measure and display the inlet water flow rate.

3.1 The Open Loop Model

The state equation with dead time in deviation form is expressed as follows:

$$\tau_1 \frac{d\Gamma_2(t-t_D)}{dt} + \Gamma_2(t-t_D) = K_1 F(t-t_D) + K_2 \Gamma_1(t-t_D) + K_3 Q_{e1}(t-t_D) \quad (1)$$

where: process gains: $K_1 \left[\frac{(^{\circ}\text{C})(\text{minute})}{\text{L}} \right]$, K_2 (dimensionless), $K_3 \left[\frac{(\text{minute})(^{\circ}\text{C})}{(\text{k})} \right]$ and process time constant: τ_1 [minute] are defined as follows:

$$K_1 = \frac{T_1 - T_2}{f} \quad (2)$$

$$K_2 = \frac{f}{f} = 1 \quad (3)$$

$$K_3 = \frac{1}{f \rho c_p} \quad (4)$$

$$\tau_1 = \frac{V_1}{f} \quad (5)$$

The flow rate $F(t)$, temperatures $\Gamma_1(t)$ and $\Gamma_2(t)$, and electric heating energy $Q_{e1}(t)$ in deviation term are expressed as follows:

$$F(t) = f(t) - \bar{f} \quad (6)$$

$$\Gamma_1(t) = T_1(t) - \bar{T}_1 \quad (7)$$

$$\Gamma_2(t) = T_2(t) - \bar{T}_2 \quad (8)$$

$$Q_{e1}(t) = q_{e1}(t) - \bar{q}_{e1} \quad (9)$$

where \bar{f} is the initial water flow rate, \bar{T}_1 and \bar{T}_2 are the initial temperatures of stream-1 and stream-2, and \bar{q}_{e1} is the initial electric heating energy of Tank-1. The Laplace transform of Equation (1) is

$$\Gamma_2(s) = \frac{K_1 e^{-t_D s}}{\tau_1 s + 1} F(s) + \frac{K_2 e^{-t_D s}}{\tau_1 s + 1} \Gamma_1(s) + \frac{K_3 e^{-t_D s}}{\tau_1 s + 1} Q_{e1}(s) \quad (10)$$

3.2 Confidence Level (CL)

The confidence level (CL) indicates the degree of correlation between the open-loop model and the laboratory observation data, ranging from 0 to 100%. A higher CL value reflects greater confidence in the model. A high CL demonstrates the reliability of the open-loop model and its suitability for control system design applications (Hermawan et al., 2024). The CL for the open-loop model is given as follows:

$$\text{CL} = 1 - \text{abs}(T_2^{\text{lab}} - T_2^{\text{model}}) \quad (11)$$

3.3 Process Reaction Curve (PRC)

PID parameters can be tuned in the laboratory using an open-loop test by manually applying a step change to the manipulated variable (MV). This method is simple and can be implemented with basic equipment (Hermawan et al., 2024). The open-loop response typically exhibits a sigmoidal characteristic, known as the process reaction curve (PRC). PRC can be approximated by a first-order-plus-dead-time (FOPDT) model (Smith and Corripio, 1997; Camacho and Smith, 2000; Hermawan and Haryono, 2012; Espin et al., 2024; Hermawan et al., 2024) as follows:

$$G_{PRC}(s) = \frac{\Gamma_2(s)}{Q_{e1}(s)} = \frac{K_{PRC} e^{-t_D s}}{t_p s + 1} \quad (12)$$

Gain K_{PRC} , time constant t_p , and time delay t_D can be determined as follows:

$$K_{PRC} = \frac{\Delta CV}{\Delta MV} = \frac{\Delta T_2}{\Delta q_{e1}} \quad (13)$$

$$t_p = \frac{3}{2}(t_2 - t_1) \quad (14)$$

In this work, times t_1 and t_2 are determined based on the CV response result. The PRC parameters (K_{PRC} , t_p , t_D) are used to calculate the PID values (K_c , τ_i , τ_D) through tuning methods such as Ziegler–Nichols, as shown in **Table 1** (Smith dan Corripio,1997).

Table 1: Ziegler-Nichols model.			
Controller	K_c	τ_i	τ_D
P	$\frac{1}{K_{PRC}} \frac{t_p}{t_D}$		
PI	$\frac{0.9}{K_{PRC}} \frac{t_p}{t_D}$	$3.3t_D$	
PID	$\frac{1.2}{K_{PRC}} \frac{t_p}{t_D}$	$2.0t_D$	$0.5t_D$

3.4 Feedback Controller

The transfer function of the conventional PID feedback controller is given as follows:

$$G_c(s) = \frac{Q_{e1}(s)}{E(s)} = K_c + \frac{K_c}{\tau_i s} + K_c \tau_D s \quad (15)$$

Error (E) can calculated as follows:

$$E(s) = \Gamma_2^{SP}(s) - \Gamma_2(s) \quad (16)$$

3.5 Smith Predictor (SP)

To eliminate the effect of dead time, the open-loop feedback signal is adjusted to carry current information rather than delayed information (Hermawan et al., 2024). The current output/information is denoted as $\Gamma_2^*(s)$ and expressed as follows:

$$\Gamma_2^*(s) = G_c(s)G_p(s)\Gamma_2^{SP}(s) \quad (17)$$

Equation (17) is obtained by adding the following term:

$$\Gamma_2^*(s) = (1 - e^{-t_d s})G_c(s)G_p(s)\Gamma_2^{SP}(s) \quad (18)$$

Therefore:

$$\Gamma_2^*(s) + \Gamma_2(s) = \Gamma_2^*(s) \quad (19)$$

A dead-time compensator (Smith predictor) estimates the delay effect of the manipulated variable on the process output using a prediction model. This method is effective only if the process transfer function and dead time are accurately known (Stephanopoulos, 1984).

3.6 Internal Model Control (IMC)

IMC has become a widely adopted method for improving control performance in process systems with dead time, particularly in the chemical industry. IMC employs model inversion with low-pass filtering to deliver systematic control design that ensures rapid and robust response in first-order plus dead time systems (Morari and Zafriou, 1989). IMC modeling follows (Seborg et al., 2017). For simplicity, the transfer functions of the measurement device and control valve are assumed as $G_M(s) = G_V(s) = 1$. The process model is represented as $G(s) = G_p(s)e^{-t_D s}$. The approximated model $\tilde{G}(s)$ is a FOPDT transfer function as follows:

$$\tilde{G}(s) = \frac{K e^{-t_D s}}{\tau s + 1} \quad (20)$$

In general, $\tilde{\Gamma}_2 \neq \Gamma_2$ because $\tilde{G}(s) \neq G(s)$. The IMC block diagram will be equivalent to the conventional FBC block diagram if the controllers $G_c(s)$ and $G_c^*(s)$ satisfy the following equation:

$$G_c = \frac{G_c^*}{1 - G_c^* \tilde{G}} \quad (21)$$

The IMC transfer function $G_c^*(s)$ is written as follows:

$$G_c^*(s) = \frac{(1 + \frac{t_D}{\tau} s)(\tau_1 s + 1)}{K(\tau_c s + 1)} \quad (22)$$

where τ_c is the desired closed-loop time constant. In this study, for robust control, τ_c is taken as three times t_D , i.e., $\tau_c = 3t_D$ (Seborg et al., 2017).

3.7 Controller Performance

An identical disturbance system was constructed to evaluate the effectiveness of all control strategies. Closed-loop error integrals after input disturbance adjustments were computed to assess performance. The integral absolute error (IAE) criterion was employed to compare controller performance quantitatively, defined as follows:

$$IAE = \int_0^t |\varepsilon(t)| dt \quad (23)$$

where the error ε is defined in the time domain and expressed as follows:

$$\varepsilon(t) = T_2^{SP} - T_2(t) \quad (24)$$

4. FINDINGS AND DISCUSSION

4.1 The Open Loop Experiment Results

The open-loop experiment was conducted to obtain the steady-state operating conditions of the stirred tank heater, which serve as the baseline for subsequent control design and evaluation. As summarized in **Table 2**, the inlet flowrate was maintained at 6 L/min with an inlet water temperature of 26.5 °C, while the outlet temperature stabilized at 28.7 °C under an electric heating input of 54 kJ/min. These results confirm that the system responds with a measurable temperature rise of 2.2 °C across the tank under steady heating, indicating a balance between the heat supplied and the thermal load carried by the continuous inflow. With a tank volume of 7.9 L, water density of 0.997 kg/L, and specific heat capacity of 4.186 kJ/kg·°C, the thermal capacity of the system can be quantified, allowing for accurate modeling of energy accumulation and dissipation. Importantly, the open-loop response highlights the inherent delay between energy input and outlet temperature change, reflecting the system's dead time characteristics. This behavior justifies the need for advanced control strategies, such as PID-SP and PID-IMC, to overcome the limitations of conventional PID tuning in processes where dead time significantly impacts control performance.

As shown in **Table 3**, the steady-state parameters obtained from the laboratory data confirm the suitability of the FOPDT model for the stirred tank heater. The negative flow rate gain ($K_1 = -0.36$ °C·min/L) highlights the dilution effect of increased inflow, while the heater gain ($K_3 = 0.040$ °C·min/kJ) quantifies the system's heating efficiency. The process time constant ($\tau_1 = 1.32$ min) and dead time ($t_D = 0.35$ min) indicate a relatively rapid but delayed response, which is critical for control tuning. These findings highlight the necessity of accounting for dead time to ensure stable and effective control performance.

Table 2: Steady state variables		
No	Steady state variable	Value
1	Tank-1 inlet flowrate, f [$\frac{L}{minute}$]	6
2	Tank-1 inlet temperature, T_1 [°C]	26.5
3	Tank-1 outlet temperature, T_2 [°C]	28.7
4	Tank-1 electric heating energy, [$\frac{kJ}{minute}$]	54
5	Tank-1 volume, V_1 [L]	7.9
6	Water density, ρ [$\frac{kg}{L}$]	0.997
7	Water heat capacity, C_p [$\frac{kJ}{kg \cdot ^\circ C}$]	4.186

Table 3: Steady state parameter		
No	Steady state parameter	Value
1	Tank-1 inlet flowrate gain, K_1 [$\frac{(^{\circ}C)(minute)}{L}$]	-0.36
2	Tank-1 inlet temperature gain, K_2 [dimensionless]	1
3	Tank-1 electric heater gain, K_3 [$\frac{(minute)(^{\circ}C)}{(kJ)}$]	0.040
4	Tank-1 process time constant, τ_1 [minutes]	1.32
5	Dead time in the measurement point, t_D [minute]	0.35

Table 4: Confidence Level (CL)	
Disturbance	CL
F increase	97.52%
F decrease	97.56%

Figure 2 shows the open-loop XCOS diagram of the stirred tank heater with dead time. At steady state, the simulated outlet temperature and gains matched the laboratory results in **Tables 2–3**, confirming the FOPDT

model and the proper implementation of transport delay. The saved time series were then used to validate the model and to initialize closed-loop simulation for PID-SP and PID-IMC.

Figure 3 shows that the model response is in close agreement with the laboratory data for both increasing and decreasing flow disturbances. The outlet temperature decreases when the flow rate increases and rises when the flow rate decreases, with both responses reflecting the measured dead time of 0.35 min. Minor deviations observed during the transient phase are likely due to experimental disturbances, yet the model successfully captures the essential dynamic characteristics, including transient behavior, steady-state values, and overall trends. The confidence levels (CL) in Table 4 further reinforce this visual agreement, reaching 97.52% for flow increase and 97.56% for flow decrease. Such high CL values confirm that the developed FOPDT model provides a reliable representation of the real process under open-loop conditions and is sufficiently accurate to serve as a foundation for control system design and analysis.

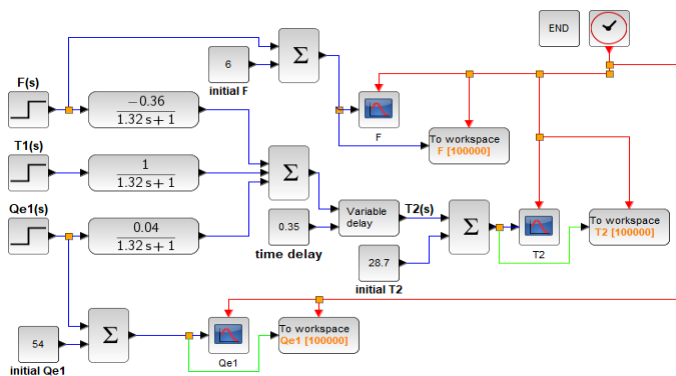


Figure 2: The open-loop XCOS diagram.

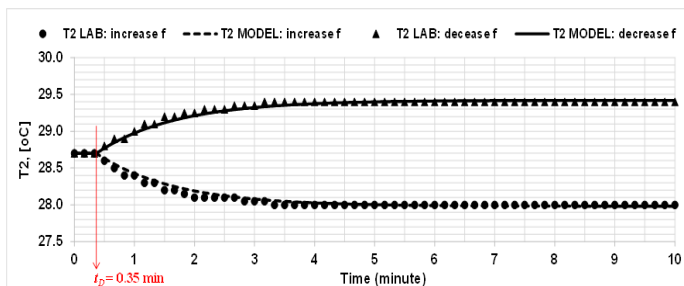
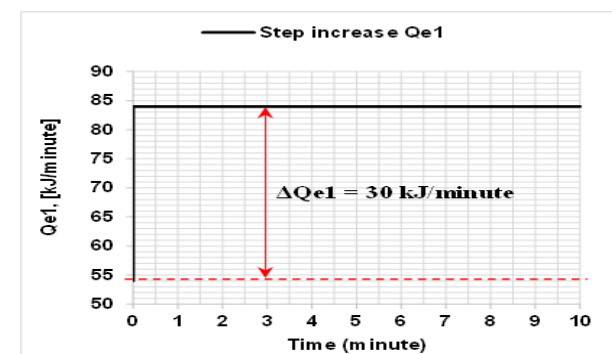


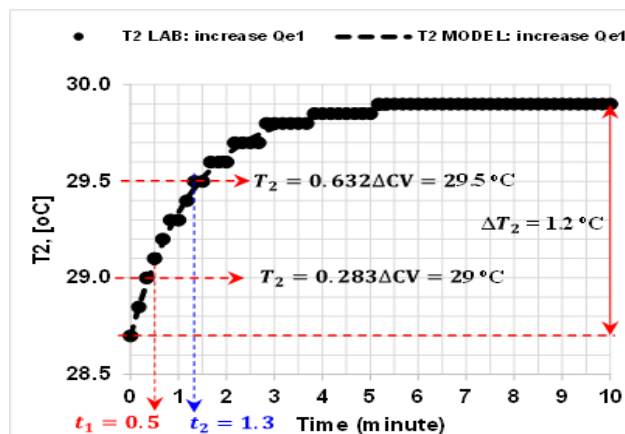
Figure 3: The open loop response to the flow disturbance changes.

4.2 Tuning Experiment Results

Figure 4 shows the process reaction curve obtained from a step increase of 30 kJ/min in heater input. The outlet temperature increased by about 1.2°C, with a measured dead time of 0.5 min and a time constant of 1.3 min. The close match between laboratory and model responses confirms the suitability of the FOPDT model for PID tuning. The PRC tuning results for PID-SP are listed in Table 5. Since the PRC tuning was unsuitable for PID-IMC, the controller was retuned using trial and error to achieve a faster and more stable response. Table 6 presents the retuned results, which demonstrate the improved performance.



(a) MV: $q_{e1}(t)$



(b) CV: $T_2(t)$

Figure 4: Process Reaction Curve for tuning of PID parameters

Table 5: PRC tuning results for the regulatory control of PID-SP.

Controller	$K_c \left[\frac{\text{kJ}}{\text{°C} \cdot \text{minute}} \right]$	τ_i [minute]	τ_D [minute]
P-SP	300		
PI-SP	270	0.33	
PID-SP	360	0.20	0.05

Table 6: Tuning parameters for the regulatory control of PID-IMC.

Controller	$K_c \left[\frac{\text{kJ}}{\text{°C} \cdot \text{minute}} \right]$	τ_i [minute]	τ_D [minute]
P-IMC	100		
PI-IMC	100	1.2	
PID-IMC	100	1.2	0.01

4.3 Closed Loop Simulation Results

Closed-loop XCOS simulations in regulatory and servo modes were performed to validate the robustness and tuning effectiveness of the PID-based control strategy. The closed-loop XCOS diagrams for PID-SP and PID-IMC are shown in Figures 5 to 10.

4.3.1 Regulatory case

Figure 11 illustrates the applied flow disturbance (regulatory mode) used to evaluate the robustness of the control configurations. Initially, the inlet flow rate is maintained at 8 L/min until minute 6, after which it is suddenly decreased to 4 L/min and held constant for the remainder of the simulation. This step disturbance serves as a critical test condition for the stirred tank heater with dead time, as it represents a significant variation in the process input. This disturbance tests how well the proposed controllers (PID-SP and PID-IMC) reject input variations and maintain stability. The responses show how effectively each configuration handles sudden process changes while keeping the system stable.

Figure 12 presents the comparative closed-loop responses of PID-SP and PID-IMC. In the CV responses, both controllers are able to track setpoint changes and compensate for flow disturbances. PID-SP produces smoother dynamics with less oscillation, while PID-IMC responds faster but with higher oscillatory behavior. For the MV responses, PID-IMC shows more stable and moderate energy adjustments, whereas PID-SP exhibits sharper fluctuations after the disturbance. However, when considering the Integral Absolute Error (IAE) results in Table 7, PID-IMC achieves the lowest IAE value (208.24), indicating superior overall performance compared to PID-SP (271.41). This result confirms that, despite its slightly more oscillatory CV behavior, PID-IMC provides a faster response with better accuracy and disturbance rejection efficiency.

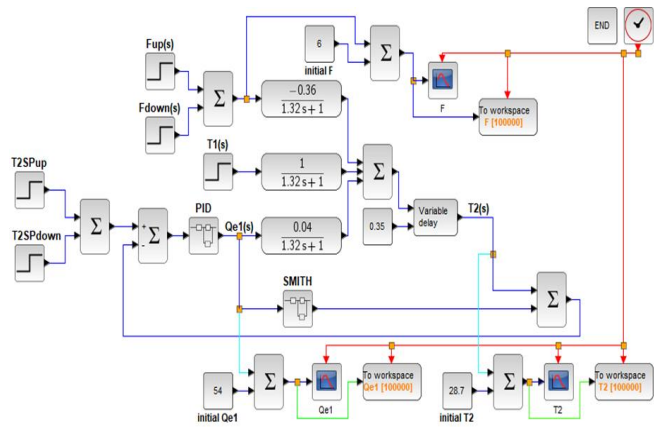


Figure 5: PID-SP XCOS diagram.

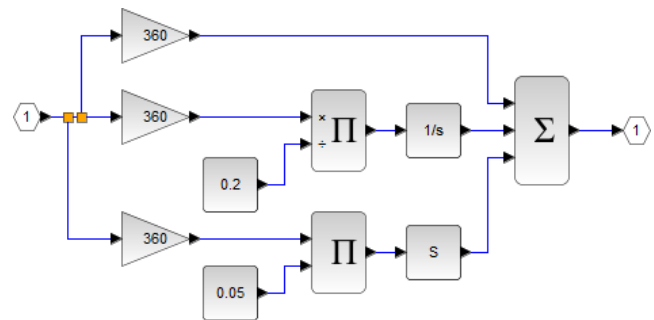


Figure 6: PID Sub-XCOS diagram in PID-SP.

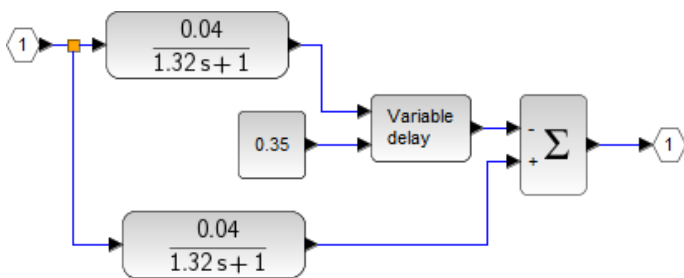


Figure 7: SP Sub-XCOS diagram in PID-SP.

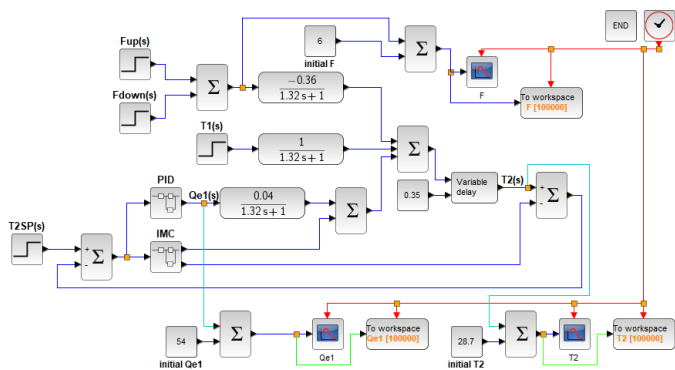


Figure 8: PID-IMC XCOS diagram.

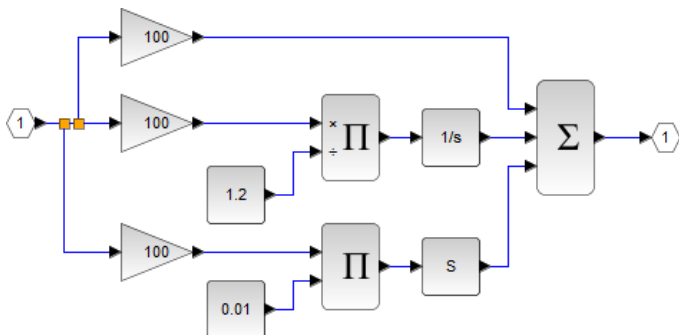


Figure 9: PID Sub-XCOS diagram in PID-IMC

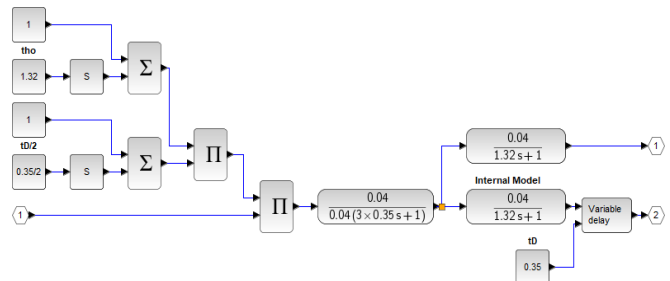


Figure 10: IMC Sub-XCOS diagram in PID-IMC.

IMC is a model-based control strategy that uses an internal process model to predict plant dynamics and proactively correct control loop errors. By combining model inversion with a low-pass filter, IMC achieves a balance between rapid response and robustness, even under model mismatch. This systematic and straightforward design approach is particularly effective for first-order plus dead time (FOPDT) systems (Morari and Zafriou, 1989). IMC provides an effective solution to mitigate stability loss and transient response degradation that often occur when dead time is significant, a condition frequently observed in real plants (Seborg et al., 2017). IMC enhances stability and output performance in dead-time processes, even under nonlinear and slow dynamics (Juneja et al., 2010; Seborg et al., 2017). It provides effective dead-time compensation and disturbance rejection beyond the capability of conventional PID control, making it practical for modern chemical process industries (Kravaris and Wright, 1989; Espin et al., 2024).

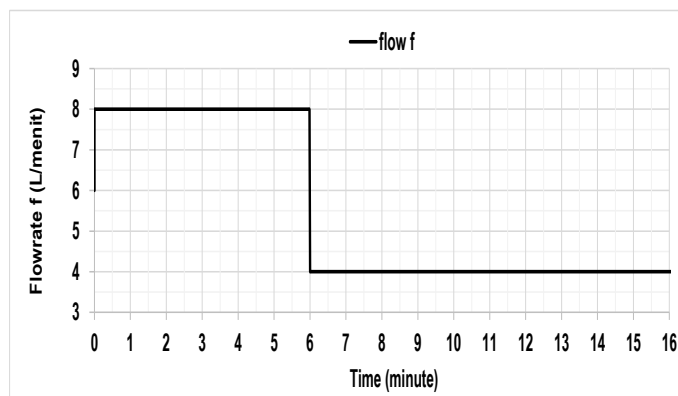


Figure 11: Flow disturbance system.

Table 7: IAE results for regulatory case.

Controller	IAE	Controller	IAE
P-SP	1295.92	P-IMC	2654.92
PI-SP	282.64	PI-IMC	221.76
PID-SP	271.41	PID-IMC	208.24

Table 8: Tuning parameters for the servo control of PID-SP and PID-IMC.

Controller	$K_c \left[\frac{kJ}{^{\circ}C \cdot minute} \right]$	τ_i [minute]	τ_D [minute]
P-IMC	50		
PI-IMC	50	1.5	
PID-IMC	50	1.5	0.03

4.3.2 Servo case

For the servo control case (set point change), where the outlet temperature (T_2) is intentionally varied, the controller parameters were retuned by trial and error to produce a faster and tighter response. The tuning results are shown in **Table 8**, which lists the proportional gain (K_c), integral time (τ_i), and derivative time (τ_d) used for each controller. The proportional gain was kept constant at 50 to ensure a fair comparison between both configurations, while the integral and derivative times were adjusted to fine-tune the response. Adding integral and derivative action improved steady-state accuracy and reduced overshoot, consistent with reported benefits of IMC-based PID tuning and analytic IMC-PID design methods (Wang et al., 2016; Castellanos-Cárdenas, et al., 2020).

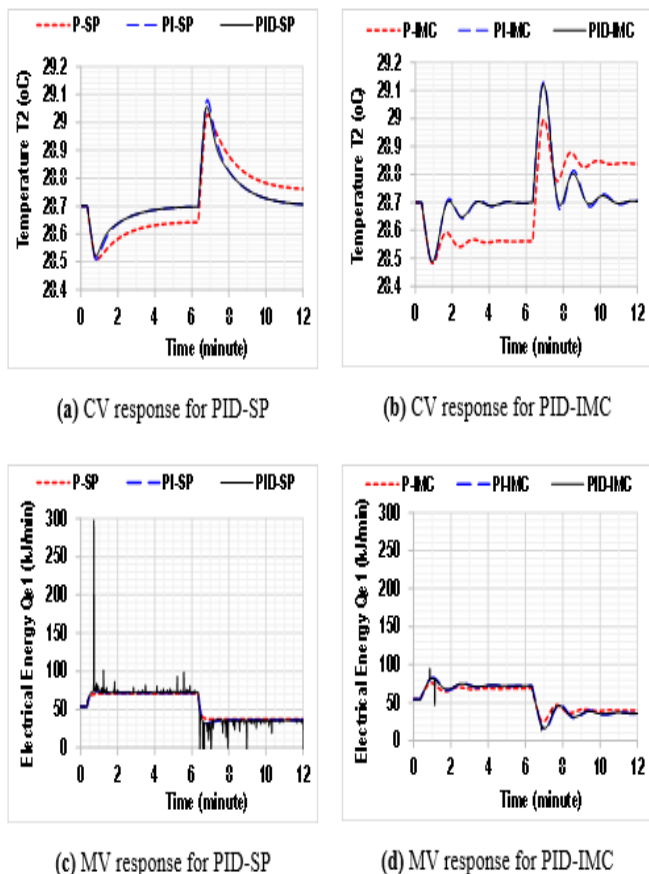


Figure 12: Comparative responses between PID-SP and PID-IMC: regulatory case.

In this experiment, the set point of T_2 was increased by 1°C at $t = 0$ minutes and decreased by 1°C at $t = 6$ minutes. **Figures 13(a)** and **13(b)** show the resulting controlled variable (CV) responses. Both PID-SP and PID-IMC controllers successfully tracked the set-point changes, but their behaviors differed. The P controller in both configurations left a noticeable steady-state offset, while the PI and PID controllers completely eliminated it. Between the two, PID-IMC achieved a faster rise and settling time, indicating stronger responsiveness and better adaptability. However, the faster action of PID-IMC results in slightly higher oscillations during the transient period, a common trade-off reported in IMC-based designs, where responsiveness is prioritized over conservatism (Jin and Liu, 2014; Castellanos-Cárdenas, et al., 2020).

The manipulated variable (MV) responses, represented by the electrical energy input (Q_{e1}) in **Figures 13(c)** and **13(d)**, show how the controllers adjust heating power. Both controllers kept the energy signals within reasonable limits, but their patterns were distinct. The PID-SP configuration generated sharper transients and brief spikes in energy, reflecting a more aggressive control effort. On the other hand, PID-IMC produced smoother and more stable control actions, which are advantageous for real systems since they reduce actuator stress and energy fluctuations. This observation is consistent with recent studies reporting that IMC-based PID tuning can smooth actuator signals and improve energy-related performance in thermal systems (Castellanos-Cárdenas, et al., 2020; Jeon and Lee, 2025).

The quantitative comparison based on the Integral Absolute Error (IAE)

values, presented in **Table 9**, supports these observations. The PID-IMC achieved the smallest IAE of **298.28**, outperforming the PID-SP's value of **505.41**. This indicates that PID-IMC provided more accurate tracking with smaller overall deviation from the set point. Similar reductions in IAE and improved tracking with IMC-based PID tuning have been reported in recent studies, while reviews and comparative analyses highlight that IMC methods typically achieve better nominal performance but require accurate models for robustness (Kumar, 2016; Castellanos-Cárdenas et al., 2020; Ningsih et al., 2024; da Silva et al., 2020).

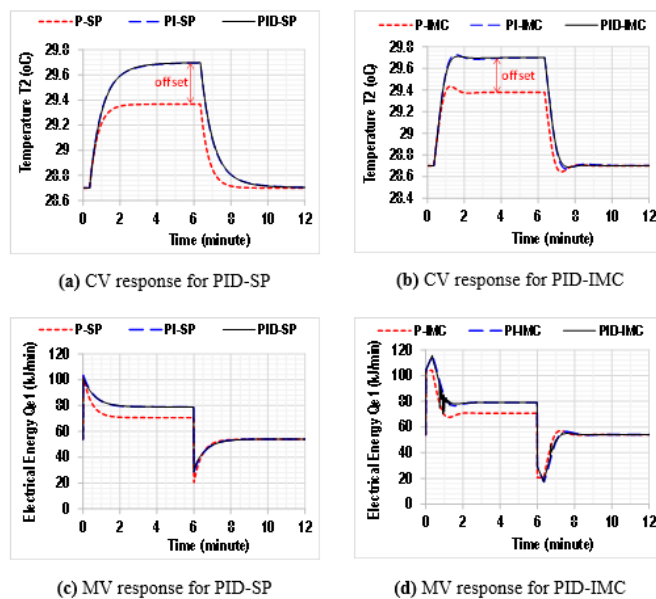


Figure 13: Comparative responses between PID-SP and PID-IMC: servo case.

Table 9: IAE results for servo case.			
Controller	IAE	Controller	IAE
P-SP	581.33	P-IMC	525.14
PI-SP	508.55	PI-IMC	310.38
PID-SP	505.41	PID-IMC	298.28

In summary, both controller configurations performed well in the servo test, but PID-IMC consistently demonstrated better accuracy, faster settling, and smoother actuator behavior. These results highlight the advantage of the IMC-based tuning method, showing that it can achieve high precision and stable performance even in systems with inherent dead time, such as the stirred-tank heater process studied here.

When the results from the servo and regulatory tests are compared, a consistent pattern emerges regarding the performance of the two controller configurations. Under disturbance rejection (regulatory) conditions, the PID-IMC achieved the smallest IAE value and demonstrated a faster and more robust response than PID-SP, though with slightly higher oscillations. In the servo control tests, this trend was confirmed: the PID-IMC again produced the lowest IAE and the quickest response while maintaining smooth manipulated-variable behavior. Similar conclusions have been reported in recent studies comparing IMC-based and Smith Predictor schemes, where IMC offers superior disturbance rejection, robustness, and smoother actuator action (Castellanos-Cárdenas et al., 2020; da Silva et al., 2020). By embedding a predictive internal model within the control structure, PID-IMC enhances the system's ability to anticipate and correct process deviations, whereas PID-SP relies primarily on reactive feedback compensation.

Overall, the combined results show that the PID-IMC offers superior dynamic performance, robustness, and energy efficiency, making it a more suitable choice for thermal systems with transport delay. Meanwhile, PID-SP remains advantageous for applications prioritizing smoother process outputs with minimal oscillation. The complementary nature of these two strategies highlights how appropriate tuning and control structure selection can significantly influence the trade-off between responsiveness and stability in process control design.

4.4 Sensitivity Analysis of Dead Time on Controller Performance

4.4.1 Regulatory case

To further assess controller robustness, the effect of dead time on closed-loop responses was analyzed for the regulatory control case. In this case, the flow rate f is increased by 2 L/min at time $t=0$. Again, the PID parameters were retuned by trial and error to achieve the stable and fast responses. **Table 10** shows the tuning parameters for this analysis. Both PID-SP and PID-IMC were tested with different dead times ($t_D = 1, 2,$ and 4 minutes) while keeping the proportional, integral, and derivative settings the same. The resulting temperature (controlled variable, T_2) and energy input (manipulated variable, Q_{e1}) responses are illustrated in **Figure 14**, while the corresponding IAE results are presented in **Table 11**.

Table 10: Tuning parameters of PID-SP and PID-IMC for dead-time sensitivity analysis.			
Controller	$K_c \left[\frac{\text{kJ}}{\text{°C} \cdot \text{minute}} \right]$	τ_i [minute]	τ_D [minute]
P-IMC	12		
PI-IMC	12	1.5	
PID-IMC	12	1.5	0.03

As shown in **Figure 14(a-d)**, increasing dead time significantly affects the dynamic performance of both control systems. For smaller delays ($t_D = 1$ minute), both controllers exhibit stable responses with minimal overshoot and quick recovery to steady state. However, as the dead time increases to 2 and 4 minutes, the control performance degrades notably—especially for PID-IMC. The PID-SP configuration shows gradual damping and moderate oscillations, indicating its ability to maintain relative stability under delayed feedback. In contrast, the PID-IMC configuration becomes increasingly oscillatory and less stable at higher dead times due to its stronger dependence on accurate process model prediction. This behavior confirms that IMC-based controllers, while highly effective under well-modeled conditions, are more sensitive to model mismatch and delay uncertainty than Smith Predictor-based controllers.

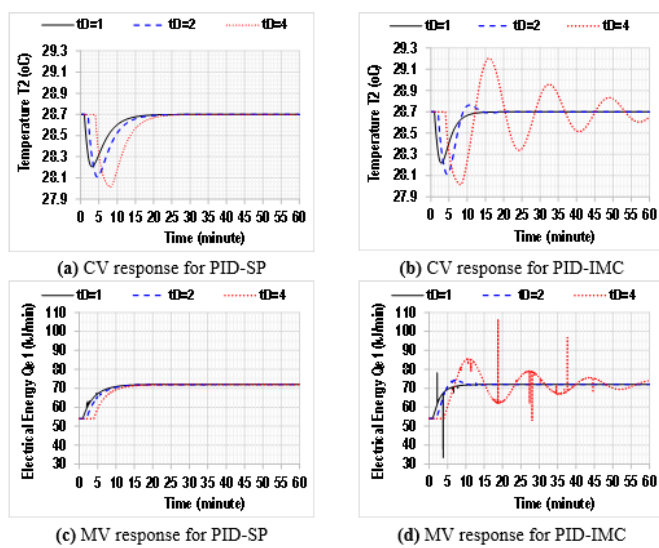


Figure 14: The influence of dead time on the closed-loop responses: Comparative responses between PID-SP and PID-IMC for the regulatory control case.

t_D (minute)	IAE	
	PID-SP	PID-IMC
1	1,017	582
2	1,538	863
4	2,970	15,717

The quantitative results in **Table 11** reinforce these observations. The IAE values for PID-SP increase steadily with dead time—from 1,017 at $t_D = 1$ minute to 2,970 at $t_D = 4$ minutes—indicating reduced control accuracy

but preserved stability. Conversely, the IAE for PID-IMC increases dramatically, from 582 to 15,717, suggesting that prediction errors due to unmodeled dead time severely impair its regulation capability. This demonstrates that while PID-IMC provides superior performance under nominal conditions, its robustness deteriorates rapidly when the actual process delay deviates from the modeled value. The PID-SP configuration, on the other hand, offers more tolerant behavior to delay variations, making it a more reliable choice for processes where dead time is uncertain or variable. These trends agree with recent studies that document IMC-PID sensitivity to model/dead-time mismatch and demonstrate the relative delay-tolerance of Smith-Predictor and filtered-Smith variants in experimental and application studies (Jin, 2014; Castellanos-Cárdenas et al., 2020; Mejía et al., 2022; Gyürkés, 2023).

Overall, the analysis highlights the trade-off between performance and robustness: PID-IMC achieves the best results when the model is accurate and delay is small, whereas PID-SP maintains better resilience under increasing dead time. This finding aligns with the study's broader conclusion that controller selection should be guided not only by steady-state performance but also by the expected variability of process dynamics.

4.4.2 Servo case

The PID tuning parameters for the servo control system are as listed in Table 10. The results presented in Figure 15 and Table 12 illustrate the effect of varying dead time ($t_D = 1, 2,$ and 4 minutes) on the servo control performance of the two controller configurations. As shown in Figures 15(a) and 15(c), the PID-SP configuration maintains a consistent and stable closed-loop response across different dead-time conditions. The controlled variable (T_2) gradually approaches the set point with minimal overshoot and no oscillation, indicating strong robustness to increasing process delay. The manipulated variable (Q_{e1}) shows smooth, monotonic responses, indicating that the Smith Predictor successfully compensates for time delay by predicting the process output. These observations align with recent findings on Smith Predictor-based control: its core advantage lies in isolating the delay effect and preserving dynamic stability even when delay grows (Normey-Rico et al., 2022; Mejía et al., 2022).

In contrast, the PID-IMC configuration (**Figures 15(b)** and **15(d)**) exhibits greater sensitivity to increasing dead time. While the IMC-based controller performs excellently under short delays ($t_D = 1$ minute), providing a fast and accurate response, the performance deteriorates as the delay increases to 2 and 4 minutes. The controlled variable displays higher overshoot and oscillatory behavior, while the manipulated variable fluctuates more aggressively. This occurs because IMC relies on an internal process model to predict system behavior, and as the dead time becomes larger or deviates from the modeled value, prediction accuracy declines. Consequently, the control action becomes less coordinated with the actual process response, leading to oscillations and instability. These behaviors align with findings in the literature: IMC-PID approaches achieve excellent nominal performance, but their robustness diminishes rapidly under significant model or delay mismatch (Jin, 2014; da Silva et al., 2020).

The quantitative comparison in **Table 12** further emphasizes these trends. For the smallest dead time ($t_D = 1$ minute), PID-IMC achieved an IAE of 387, much lower than the PID-SP's 835, indicating superior tracking accuracy. However, as the dead time increased, the IAE for PID-IMC rose sharply, reaching 667 for $t_D = 2$ minutes and an extremely high 20,020 for $t_D = 4$ minutes, showing severe degradation of performance. In contrast, the PID-SP maintained relatively moderate IAE growth (from 835 to 1,847), confirming its robustness in the presence of large dead times. These findings are in line with theory and previous research, showing that the Smith Predictor performs better than IMC when there's a large delay or model uncertainty. These findings align with recent research showing that IMC-PID controllers deliver excellent accuracy when the process model is valid but deteriorate rapidly under dead-time or model mismatch, while Smith Predictor and related compensators maintain greater stability under uncertainty (Jin, 2014; da Silva et al., 2020; Morgan and McMillan, 2025).

In summary, the servo control results reveal a clear performance trade-off between the two configurations. PID-IMC offers superior accuracy and faster set-point tracking under low-dead-time and well-modeled conditions, but its performance deteriorates rapidly as delay increases. Conversely, PID-SP provides more stable and consistent control across a wider range of dead-time conditions, albeit with slower response and higher steady-state IAE for small delays. Therefore, choosing between IMC and the Smith Predictor should depend on the process features, especially the size and uncertainty of the delay, to achieve the best balance between speed and stability.

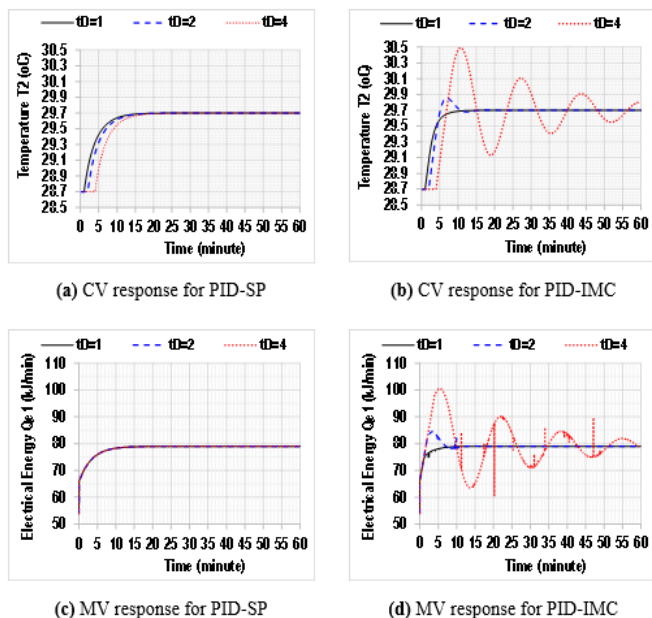


Figure 15: The influence of dead time on the closed-loop responses: Comparative responses between PID-SP and PID-IMC for the servo control case.

Table 12: The influence of dead time on IAE results for the servo control case.

t_d (minute)	IAE	
	PID-SP	PID-IMC
1	835	387
2	1,113	667
4	1,847	20,020

5. CONCLUSION

This study presented a comparative experimental evaluation of two advanced control configurations—PID with Smith Predictor (PID-SP) and PID with Internal Model Control (PID-IMC)—implemented on a two-tank thermal system with transport delay. Both controllers effectively maintained temperature regulation and exhibited satisfactory performance in set-point tracking. However, their dynamic characteristics diverged under varying delay conditions. The PID-SP configuration demonstrated superior robustness to delay variations and model mismatches, maintaining stable operation across a range of conditions. In contrast, the PID-IMC configuration achieved faster and more accurate tracking when the process model was precise, but its performance degraded significantly under increased or uncertain delay.

The principal novelty of this work lies in its experimental validation and systematic quantitative comparison of PID-SP and PID-IMC performance under multiple dead-time scenarios within a coupled thermal process. The results offer fresh empirical data regarding the trade-off between model-based responsiveness (IMC) and robust delay compensation (Smith Predictor), elucidating their respective benefits in practical thermal control scenarios. This contribution strengthens the understanding of how predictive model accuracy and dead-time uncertainty jointly influence the stability and efficiency of industrial thermal systems.

LIMITATION AND FURTHER RESEARCH

This study was carried out on a laboratory-scale two-tank thermal system with constant model parameters, limiting its applicability to real processes where nonlinearities, parameter drift, and measurement delays are present. The FOPDT-based model used for controller design may not fully represent multivariable or nonlinear heat transfer behavior. Sensitivity analysis showed that PID-IMC performance degrades under significant model mismatch or large dead-time variations, indicating reduced robustness under non-nominal conditions. Future studies should explore ways to improve adaptability and delay handling—like adaptive tuning, hybrid IMC-MPC control, or data-driven methods—to boost performance in real, large-scale thermal systems.

ACKNOWLEDGMENTS

The authors sincerely acknowledge the financial assistance from LPPM UPN 'Veteran' Yogyakarta through contract number 404/UN62.21/PG.00.00/2025. Gratitude is extended to the Department of Chemical Engineering, UPN 'Veteran' Yogyakarta, for granting access to the Process and Product Systems Development Research Laboratory. The availability of free software, Scilab and XCOS, also provided valuable technical support in conducting this research.

REFERENCES

Alvaro, R. J., Maria, D., and F. B., D. 2018. Level control in a system of tanks in interacting mode using Xcos software. *Contemporary Engineering Sciences*, 11, 63–70. <https://doi.org/10.12988/ces.2018.712206>

Camacho, O., and Smith, C. A. 2000. Sliding mode control: An approach to regulate nonlinear chemical processes. *ISA Transactions*, 39(2), 205–218. [https://doi.org/10.1016/S0019-0578\(99\)00043-9](https://doi.org/10.1016/S0019-0578(99)00043-9)

Castellanos-Cárdenas, D., Castrillón, F., Vásquez, R. E., and Smith, C. 2020. PID tuning method based on IMC for inverse-response second-order plus dead time processes. *Processes*, 8(9), 1183. <https://doi.org/10.3390/pr8091183>

da Silva, L. R., Flesch, R. C. C., and Normey-Rico, J. E. 2020. Controlling industrial dead-time systems: When to use a PID or an advanced controller. *ISA Transactions*, 99, 339–350. <https://doi.org/10.1016/j.isatra.2019.09.008>

Divakar, K., Kumar, M. P., Dhanamjayulu, C., and Gokulakrishnan, G. 2024. A technical review on IMC-PID design for integrating process with dead time. *IEEE Access*, 12, 124845–124870. <https://doi.org/10.1109/ACCESS.2024.3453828>

Espin, J., Camacho, C., and Camacho, O. 2024. Control of non-self-regulating processes with long time delays using hybrid sliding mode control approaches. *Results in Engineering*, 22, 102113. <https://doi.org/10.1016/j.rineng.2024.102113>

Gyürkés, M., Tacsí, K., Pataki, H., and Farkas, A. 2023. Residence time distribution-based Smith predictor: An advanced feedback control for dead time-dominated continuous powder blending process. *Journal of Pharmaceutical Innovation*, 18, 1381–1394. <https://doi.org/10.1007/s12247-023-09728-3>

Hermawan, Y. D., and Haryono, G. 2012. Dynamic simulation and composition control in a 10 L mixing tank. *Reaktor*, 14(2), 95–100. <https://doi.org/10.14710/reaktor.14.2.95-100>

Hermawan, Y. D., and Puspitasari, M. 2018. Tuning of PID controller using open loop on-off method and closed loop dynamic simulation in a 10 L mixing tank. *Contemporary Engineering Sciences*, 11(101), 5027–5038. <https://doi.org/10.12988/ces.2018.810550>

Hermawan, Y. D., Yusuf, Y., Andari, E. R., Rahma, A. A., Kurniarto, M. N. T., Simanulung, V., Rahman, A. A., Majid, N., and Sulistyarto, H. B. 2024. Design of adaptive-PID-Smith control in the two-mixing tank series. *Smart Science*, 12(3), 445–461. <https://doi.org/10.1080/23080477.2024.2350818>

Jeon, T. Y., and Lee, Y. C. 2025. Energy saving in ship central cooling systems: IMC-tuned PID with feedforward control. *Journal of Marine Science and Engineering*, 13(3), 510. <https://doi.org/10.3390/jmse13030510>

Jin, Q. B., and Liu, Q. 2014. Analytical IMC-PID design in terms of performance/robustness tradeoff for integrating processes: From 2-DOF to 1-DOF. *Journal of Process Control*, 24(3), 22–32. <https://doi.org/10.1016/j.jprocont.2013.12.011>

Juneja, P. K., Ray, A. K., and Mitra, R. 2010. Various controller design and tuning methods for a first order plus dead time process. *International Journal of Computer Science & Communication*, 1(2), 161–165.

Karan, S., and Dey, C. 2023. IMC based modified Smith predictor for second order delay dominated processes with RHP. *ISA Transactions*, 142, 254–269. <https://doi.org/10.1016/j.isatra.2023.08.009>

Karan, S., Dey, C., and Mukherjee, S. 2022. Simple internal model control based modified Smith predictor for integrating time delayed processes with real-time verification. *ISA Transactions*, 121, 240–257.

- <https://doi.org/10.1016/j.isatra.2021.04.008>
- Korupu, V. L., and Muthukumarasamy, M. 2021. A comparative study of various Smith predictor configurations for industrial delay processes. *Chemical Product and Process Modeling*. <https://doi.org/10.1515/cppm-2021-0026>
- Kravaris, C., and Wright, R. A. 1989. Deadtime compensation for nonlinear processes. *AIChE Journal*, 35(9), 1535–1542. <https://doi.org/10.1002/aic.690350914>
- Kumar, D. B. S., and Sree, R. P. 2016. Tuning of IMC-based PID controllers for integrating systems with time delay. *ISA Transactions*, 63, 242–255. <https://doi.org/10.1016/j.isatra.2016.03.020>
- Luyben, W. L. 2002. *Plantwide dynamic simulators in chemical processing and control* (pp. 25–33). Marcel Dekker.
- Marlin, T. E. 1995. *Designing processes and control systems for dynamic performance* (2nd ed., pp. 97–337). McGraw-Hill.
- Mejía, C., Salazar, E., and Camacho, O. 2022. A comparative experimental evaluation of various Smith predictor approaches for a thermal process with large dead time. *Alexandria Engineering Journal*, 61(12), 9377–9394. <https://doi.org/10.1016/j.aej.2022.03.047>
- Morari, M., and Zafiriou, E. 1989. *Robust process control*. Prentice Hall.
- Morgan, P., and McMillan, G. 2025. Face-off: Smith predictor vs. dead-time compensated PID. *ControlGlobal*.
- Ningsih, W., Suharti, P. H., and Ghani, M. 2024. Performance analysis of IMC-PID controller on PCT-14 air pressure control system. *MethodsX*, 11, 102966. <https://doi.org/10.1016/j.mex.2024.102966>
- Normey-Rico, J. E., Santos, T. L. M., Flesch, R. C. C., and Torrico, B. C. 2022. Control of dead-time process: From the Smith predictor to general multi-input multi-output dead-time compensators. *Frontiers in Control Engineering*, 3, 953768. <https://doi.org/10.3389/fcteg.2022.953768>
- Panda, R. C., Hung, S. B., and Yu, C. C. 2006. An integrated modified Smith predictor with PID controller for integrator plus dead-time processes. *Industrial & Engineering Chemistry Research*, 45, 1397–1407. <https://doi.org/10.1021/ie0580194>
- Seborg, D. E., Edgar, T. F., Mellichamp, D. A., and Doyle, F. J. 2017. *Process dynamics and control* (4th ed., pp. 368–394). John Wiley & Sons.
- Smith, C. A., and Corripio, A. B. 1997. *Principles and practice of automatic process control* (2nd ed.). John Wiley & Sons.
- Stephanopoulos, G. 1984. *Chemical process control: An introduction to theory and practice*. Prentice Hall.
- Stojic, M. R., Matijevic, M. S., and Draganovic, L. S. 2001. A robust Smith predictor modified by internal models for integrating process with dead time. *IEEE Transactions on Automatic Control*, 46(8), 1293–1298. <https://doi.org/10.1109/9.940937>
- Wang, Q., Lu, C., and Pan, W. 2016. IMC-PID controller tuning for stable and unstable processes with time delay. *Chemical Engineering Research and Design*, 105, 120–129. <https://doi.org/10.1016/j.cherd.2015.11.011>

